

High-pressure synthesis, crystal structure determination, and a Ca substitution study of the metallic rhodium oxide NaRh_2O_4

Kazunari Yamaura,^{1,} Qingzhen Huang,² Monica Moldovan,³ David P. Young,³ Akira Sato,⁴ Yuji Baba,⁵
Yoshio Matsui,⁵ and Eiji Takayama-Muromachi¹*

Superconducting Materials Center, National Institute for Materials Science, 1-1 Namiki, Tsukuba,
Ibaraki 305-0044, Japan; NIST Center for Neutron Research, National Institute of Standards and
Technology, Gaithersburg, Maryland 20899; Department of Physics and Astronomy, Louisiana State
University, Baton Rouge, LA 70803; Research Promotion Division, National Institute for Materials
Science, 1-1 Namiki, Tsukuba, Ibaraki 305-0044, Japan; Advanced Materials Laboratory, National
Institute for Materials Science, 1-1 Namiki, Tsukuba, Ibaraki 305-0044, Japan

RECEIVED DATE ()

TITLE RUNNING HEAD: NaRh_2O_4 and CaRh_2O_4

* To whom correspondence should be addressed.

E-mail: YAMAURA.Kazunari@nims.go.jp; Fax. +81-29-860-4674

¹ SMC, National Institute for Materials Science

² National Institute of Standards and Technology

³ Louisiana State University

⁴ RPD, National Institute for Materials Science

⁵ AML, National Institute for Materials Science

ABSTRACT

The sodium rhodate NaRh_2O_4 was synthesized for the first time and characterized by neutron and x-ray diffraction studies, measurements of magnetic susceptibility, specific heat, electrical resistivity, and the Seebeck coefficient. NaRh_2O_4 crystallizes in the CaFe_2O_4 -type structure, which is comprised of a characteristic RhO_6 octahedra network. The compound is metallic in nature, probably reflecting the 1 to 1 mixed valence character of Rh(III) and Rh(IV) in the network. For further studies of the compound, the Rh valence was varied significantly by means of an aliovalent substitution: the full range solid solution between NaRh_2O_4 and CaRh_2O_4 was achieved and characterized as well. The metallic state was dramatically altered, and a peculiar magnetism developed in the low Na concentration range.

KEYWORDS: Inorganic compounds, Oxides, Magnetic properties, High-pressure synthesis

INTRODUCTION

One of major series of complex oxides in solid state chemistry is the 1:2 compound AB_2O_4 , which frequently represents a spinel-type group [1]. Regarding the general expression, not only the spinel group, but also other groups are incorporated into this category. For example, another major group in AB_2O_4 is the $CaFe_2O_4$ -type. The prototype $CaFe_2O_4$ crystallizes in an orthorhombic structure with lattice constants $a = 9.217 \text{ \AA}$, $b = 10.702 \text{ \AA}$, and $c = 3.018 \text{ \AA}$ (the space group is $Pnma$) [2], which is built up of eight-fold coordinated Ca atoms and distorted FeO_6 octahedra. After the first report of the synthesis of $CaFe_2O_4$ in 1956 [3], a variety of elements were found to replace Ca or Fe, and totally independent A and B elements were found crystallizing in the same structure. As far as we know, A= Ba, Sr, Ca, Mg, Na, La, Eu, and B= La, Pr, Nd, Sm, Eu, Gd, Tb, Dy, Ho, Yb, Lu, Y, Sc, In, Rh, Ti, Fe, V, Cr [2,4], Al [5], Ru [6], Mn [7,8,9], Ga [10], Tl [11] are reported for the $CaFe_2O_4$ -type group.

Even though the $CaFe_2O_4$ structure type appears to be rather common, significant attention has not been paid to this group in regards to its magnetic and the electrical properties. There are a few examples: $CaFe_2O_4$ (Fe^{3+} : $t_{2g}^3 e_g^2$, $S=5/2$) and $CaMn_2O_4$ (Mn^{3+} : $t_{2g}^3 e_g^1$, $S=2$) are anti-ferromagnetic below $\sim 160 \text{ K}$ [12] and $\sim 220 \text{ K}$ [7,8,9], respectively, and no metallic materials have been discovered thus far, except $NaRu_2O_4$ [6]. $NaTi_2O_4$ is also expected to be a metal from a mixed valence picture of Ti, however, experimental details are unavailable [13,14].

The edge and corner sharing BO_6 octahedra in the $CaFe_2O_4$ -type structure form a very distinctive network, similar to the one formed in the related perovskite materials. This structural network suggests that interesting physical properties may exist in the $CaFe_2O_4$ -type compounds, as are observed in related systems, such as high- T_c superconductivity in cuprates [15], quantum magnetic characters in ruthenates [16], and strongly correlated features in manganates [17]. Motivated by this hypothesis, we have searched a new member of the $CaFe_2O_4$ -type group, which has the active BO_6 network in a magnetic and electrical sense. Recently, $NaRh_2O_4$ was synthesized by solid-state reaction at a high temperature and pressure. The octahedra network in sodium rhodate contains both Rh^{3+} ($t_{2g}^6 e_g^0$, $S=0$) and Rh^{4+} ($t_{2g}^5 e_g^0$, $S=1/2$) at the 1 to 1 ratio; one half of the RhO_6 octahedra are in the spin-1/2 unit.

In this paper, we report synthesis, crystal structure, magnetic and electrical properties of the novel sodium rhodate, and results of studies by aliovalent substitution $\text{Na}^{1+}/\text{Ca}^{2+}$. A full range solid solution between NaRh_2O_4 and CaRh_2O_4 [18,19] was synthesized under the same condition.

EXPERIMENTAL

--SAMPLE PREPARATION.

Polycrystalline samples of $\text{Na}_{1-x}\text{Ca}_x\text{Rh}_2\text{O}_4$ ($x=0, 0.25, 0.5, 0.75, 1$) were prepared in a platinum cell (6.8 mm in diameter, 0.2 mm in thickness and approximately 5 mm in height) by solid-state reaction in a high pressure apparatus. Fine and pure powders of CaO (99.99 %), Rh_2O_3 , NaRhO_2 , and KClO_4 (99.5 %) were mixed stoichiometrically, and placed into the platinum cell. Previous to the high-pressure experiment, the Rh_2O_3 powder had been prepared from the Rh powder (99.9%) by heating in oxygen at 1000 °C overnight [20]. The powder NaRhO_2 had also been synthesized from a mixture of Na_2O_2 (98 %) and Rh (99.9 %) powders, which was heated in oxygen at 700 °C for 15 hrs, and then repeating the synthesis at 800 °C for 40 hrs [21]. The platinum cell was heated in the apparatus at 1500 °C for 1 hr at 6 GPa and then quenched at room temperature before releasing the pressure. A technical description of the high-pressure apparatus is detailed elsewhere [22,23]. The sintered samples were dense, black, and retained a pellet shape. Each face of the polycrystalline pellet was polished carefully in order to remove any possible contaminations from chemical reactions with the platinum cell. A typical sample mass was ~0.4 grams.

The samples were examined for quality with powder X-ray ($\text{CuK}\alpha$) diffraction at room temperature on a Rigaku RINT-2000 powder diffractometer, which is equipped with a graphite monochromator on the counter side. In Fig. 1, X-ray diffraction profiles for all the samples are shown. Each peak distribution clearly indicates the CaFe_2O_4 -type structure is formed in all the samples and the absence of significant impurities except KCl . Details of the qualitative analysis are in a supporting information file (see the end of text). Lattice parameters of the orthorhombic unit cell were determined by a least-squares method, and the evolution of those through the Ca substitution is plotted in Fig. 2. The evolution is

small and goes rather monotonically over the Ca/Na range: only approximately 1.7 % change is seen in the unit-cell volume.

Single crystals of CaRh_2O_4 were grown in the high-pressure apparatus. Approximately a 0.3-gram mixture of CaO , CaCl_2 , Rh_2O_3 , and KClO_4 with the ratio 1: 0.109: 0.5: 0.135, respectively, was placed into a double-layered cell consisting of aluminum oxide (inner) and platinum (outer). The sample mixture was isolated from the platinum capsule by the aluminum oxide inner layer. The sample cell was heated at 1500 °C at 6 GPa for 3 hrs, followed by quenching at room temperature before releasing the pressure. After mechanically removing the layers, a clump of small crystals appeared at the surface of the sample. The crystals were separated by brief treatment in a water sonic bath, and shiny, black crystals up to 0.1 mm in the largest dimension were obtained. The crystal was identified as CaRh_2O_4 by an X-ray method (described below). We believe a relatively small degree of temperature gradient in the sample cell between the center and the edge plays a significant role in the crystal growth. Studies to obtain crystals of the other compositions are in progress.

--CHEMICAL ANALYSIS.

A piece of polycrystalline NaRh_2O_4 was studied by an energy dispersive X-ray spectroscopy (EDS) at an acceleration voltage of 10 kV in an AKASHI ISI-DS-130 scanning electron microscope. The X-ray spectrum obtained at more than 10 points on the polished surface clearly revealed the absence of platinum contamination. More specifically, platinum was not detected at all above the background level, indicating the platinum concentration was less than 0.1 wt%. We recognized only Na, Rh, O and C (coating material) contributions to the spectra.

In a scanning image at relatively low magnification, a small amount of fragments were found randomly distributed, which exhibited a striking contrast to the major portion. Focused analysis was then conducted on the fragments and revealed the presence of K and Cl. The result is entirely consistent with what was indicated in the X-ray powder diffraction analysis. There are, therefore, no doubts about the formation of KCl residue.

Because we found a small discrepancy in the unit cell parameters between single- and poly-crystal samples of CaRh_2O_4 ; $a = 9.0354(3) \text{ \AA}$, $b = 3.0340(1) \text{ \AA}$, $c = 10.7062(3) \text{ \AA}$, and $V=293.49(2) \text{ \AA}^3$ for single-crystal and $a = 9.035(1) \text{ \AA}$, $b = 3.081(1) \text{ \AA}$, $c = 10.78(1) \text{ \AA}$, and $V=300.0(2) \text{ \AA}^3$ for poly-crystal, a thermogravimetric analysis of the polycrystalline CaRh_2O_4 was conducted. The polycrystalline CaRh_2O_4 was prepared from CaO and Rh_2O_3 without adding KClO_4 because the starting mixture was just stoichiometric. Oxygen content of the sample was studied by reduction to calcium monoxide and rhodium by heating in 3%-hydrogen/argon at a heating rate of 2°C per minute to 800°C and holding for 8 hours. The measurement was repeated three times. The weight loss data clearly revealed an oxygen-superstoichiometric composition 4.11(3) per formula unit under the synthesis condition, even though the source of the excess oxygen was uncertain. Otherwise, a possible metal deficiency was introduced in the structure as found in the Na-deficient compound $\text{Na}_{0.7}(\text{FeAl})_{0.7}\text{Ti}_{1.3}\text{O}_4$ [24]. For the single crystal, a corresponding non-stoichiometry was not detected in the X-ray refinement study (shown later). The non-stoichiometry in the polycrystalline sample could be responsible for the small discrepancy in the unit cell parameters.

-- ELECTRON DIFFRACTION ANALYSIS.

Selected samples were studied by electron diffraction (ED) on a Hitachi H-1500 electron microscope, in which the electrons were accelerated under a voltage of 820 kV. Careful studies of the compositions $\text{Na}_{0.5}\text{Ca}_{0.5}\text{Rh}_2\text{O}_4$ and $\text{Na}_{0.25}\text{Ca}_{0.75}\text{Rh}_2\text{O}_4$ by ED revealed that the unit cell was indeed orthorhombic. There were no extra reflections, either sharp or diffuse, which would indicate that there is short range or long range ordering of the Na/Ca site under the conditions of the synthesis. Representative patterns are shown in a supporting information file.

--NEUTRON DIFFRACTION ANALYSIS.

Because a single crystal of NaRh_2O_4 was thus far unavailable, we decided to conduct a neutron diffraction study on the polycrystalline NaRh_2O_4 . Approximately 1 gram of powder of the NaRh_2O_4 sample was briefly washed in a water sonic bath to remove KCl residue. The powder was then set in the BT-1 high-resolution diffractometer at the NIST Center for Neutron Research, employing a $\text{Cu}(311)$

monochromator. Collimators with horizontal divergences of 15', 20', and 7' of arc were used before and after the monochromator, and after the sample, respectively. The calibrated neutron wavelength was $\lambda = 0.15396(1)$ nm, and a drift was negligible during the data collection. Intensity of the reflections was measured at 0.05-degree steps in the 2-theta range between 3 and 168 degrees. The survey was conducted at room temperature. Neutron scattering amplitudes used in data refinements were 0.363, 0.593, and $0.581 (\times 10^{-12} \text{ cm})$ for Na, Rh, and O, respectively.

--SINGLE CRYSTAL X-RAY DIFFRACTION ANALYSIS

A selected CaRh_2O_4 crystal was mounted on the end of a fine glass fiber in an area-detector diffractometer (Bruker SMART APEX, $\text{MoK}\alpha$ $\lambda=0.71069 \text{ \AA}$). The X-ray study was conducted over night between 25 and 28 °C. Raw data consisting of 1833 frames were collected in ω scan mode at every 0.3 degrees for 30 seconds ($2\theta_{\text{max}}$ was 104.27 degrees). The SMART software was employed for data acquisition and the SAINT+ for data extraction and reduction [25]. An empirical absorption correction was applied with the program SADABS [25]. Structure analysis was attempted on the F^2 data by a full-matrix least-squares refinement with the SHELXL-97 program [26].

--PHYSICAL PROPERTIES MEASUREMENTS.

Electrical resistivity of the polycrystalline samples was measured between 2 K and 390 K by a conventional four-point method in a commercial apparatus (Quantum Design, PPMS system). The ac-gage current was 1 mA at 30 Hz. Silver epoxy was used to fix fine platinum wires ($\sim 30 \text{ }\mu\text{m}$ diameter) at four locations along each bar-shaped sample. Thermopower of the samples was measured in the PPMS system between 2 K and 300 K with a comparative technique using a constantan standard. The magnetic susceptibility was measured in a commercial apparatus (Quantum Design, MPMS-XL) at 10 kOe between 2 K and 390 K. The magnetization was studied in the apparatus at 5 K below 70 kOe. Specific-heat measurements were conducted in the PPMS system with a time-relaxation method over the temperature range between 1.8 K and 10 K.

RESULTS AND DISCUSSION

Atomic coordination and local structure environment of NaRh_2O_4 was investigated by the neutron diffraction study. A Rietveld analysis was applied on the powder diffraction profile with the GSAS program [27]. The structure parameters of CaFe_2O_4 were employed as an initial model in the refinement, which aided in obtaining a reliable solution. The best refinement result is shown in Fig. 3. The difference curve (bottom part of the figure) clearly indicates that the raw pattern was precisely reproduced by the model. The refinement details are shown in Tables I and II. In a preliminary study, we temporally unfixed the occupancy factor of Na in order to test for possible non-stoichiometric character. As a result, a very stoichiometric 0.993(24) Na per formula unit was confirmed. We, therefore, decided to fix the Na occupancy - being fully occupied in the final step.

The crystal structure view of NaRh_2O_4 was drawn on the basis of the results above (Fig. 4). The structure is nearly identical to that of the prototype compound CaFe_2O_4 ; both have the same space group and similar coordinate environments. The most characteristic feature in the structure should be the double Rh-O chain, which runs along the *b*-axis, as is sketched out at the bottom of Fig. 4. The RhO_6 octahedra are connected by edge sharing within each chain, and the chains are tied to neighbors by sharing the corner oxygen. The principal Rh—O—Rh angle in the chain is approximately 98 degrees [average of 97.15(22) and 99.79(16) degrees, see supporting information file]. The intra-chain bond may significantly influence the electrical conductivity (shown later). The inter-chain Rh—O—Rh angles are approximately 130 and 122 degrees. The one dimensional anisotropy of the electronic conducting state might not be expected for this configuration; however it would be interesting to study the degree of the conductivity anisotropy in and out of the chain once a high quality NaRh_2O_4 single crystal is available.

The sodium cobalt oxide NaCo_2O_4 crystallizes in a layered structure comprised of edge sharing CoO_6 octahedra [28]. The layered coordination is believed to play a significant role in the remarkably large thermoelectric power [29]. We were then interested in the thermoelectric properties of NaRh_2O_4 , because both 1:2 compounds share some common properties, such as the same number of d electrons per B atom and the same structure basis consisting of the edge sharing BO_6 octahedra. However, there

are structural differences between them. As the most distinguishing structural feature, the layer (NaCo_2O_4) and chain (NaRh_2O_4) types, was expected to depend on the relative ionic size of Na and Rh/Co, we considered the Kugimiya and Steinfink (KS) relation for the both compounds [30,31]. The KS relation predicts that the AB_2O_4 stoichiometry is characterized by two principal parameters: the ratio r_A/r_B (the ionic size factor) and the constant K_{AB} (the bond stretching force factor). The K_{AB} is defined as $K_{AB} = X_A X_B / r_c^2$, where $r_c^2 = (r_A + r_O)^2 + (r_B + r_O)^2 + 1.155(r_A + r_O)(r_B + r_O)$, and X_A (X_B) is the electronegativity of the A (B) ion. The r_A , r_B , and r_O are the radii of A, B, and O ions, respectively. Analyzing the rhodate material first, we obtained $r_A = 1.18 \text{ \AA}$ for Na, $r_B = 0.633 \text{ \AA}$ for Rh, $r_O = 1.4 \text{ \AA}$, $X_A = 1.01$ for Na, and $X_B = 1.45$ for Rh [31,32], and the numerical data yielded the constants $K_{AB} = 0.0869$ and $r_A/r_B = 1.87$. Although the result was slightly out of the range of the KS scheme, it is reasonable to include it in the category of the CaFe_2O_4 -type [30]. The result for CaRh_2O_4 ($K_{AB} = 0.0907$ and $r_A/r_B = 1.68$) was within the CaFe_2O_4 -type category and very close to the point for NaRh_2O_4 . The results, therefore, approximates the experimental result quite well. Second, the values for the layered compound NaCo_2O_4 were also considered, however multiple values of K_{AB} and r_A/r_B , which cover all configurations of Co^{3+} and Co^{4+} with low- and high-spin states, indicated that the compound NaCo_2O_4 was far outside of the range of the KS scheme. It was, therefore, difficult to reach a clear understanding of the role of ionic size in the structural features of NaCo_2O_4 and NaRh_2O_4 . Further studies will be needed.

To our knowledge, no studies have been reported on the structure of the calcium rhodate CaRh_2O_4 . The structure refinement study was then conducted on a single-crystal of CaRh_2O_4 . The results were compared with those of the prototype CaFe_2O_4 and the sodium rhodate NaRh_2O_4 . Details of the data collection are in Table III, and the calculated atom positions and thermal parameters are listed in Table IV. A structure distortion in CaRh_2O_4 was observed. The RhO_6 octahedra were found being distorted, but on a relatively small degree; the minimum and maximum distances between Rh and the six ligand oxygen were $1.993(1) \text{ \AA}$ and $2.054(2) \text{ \AA}$, respectively, the difference being $\sim 3.1 \%$. It is obviously smaller than 6.9% for CaFe_2O_4 [12] and roughly comparable to 2.1% for NaRh_2O_4 , and thus suggests

keeping the space group as *Pnma*. The structure of CaTi_2O_4 is a unique example that crystallizes in a lower symmetry structure than the *Pnma* type [33,34].

Next, oxygen non-stoichiometry was tested and found to be negligible, in striking contrast to the polycrystalline data as already shown (approximately 0.1 mole of excess oxygen was detected). The empirical stoichiometry of the single crystal CaRh_2O_4 is identical to that found for NaRh_2O_4 .

In Fig. 5, temperature and Ca concentration dependence of the electrical resistivity is shown. The resistivity of the title compound NaRh_2O_4 is typical of a normal metal. This might reflect the mixed Rh valence character: formally 0.5 unpaired electrons per Rh contribute to the conducting state. As the data indicate, the Ca substitution alters the conducting state dramatically. The state gradually shifts to being poorly conducting with increasing Ca concentration, and the end compound CaRh_2O_4 is indeed electrically insulating. The feature is consistent with a simple expectation from the filled t_{2g} band. Considering that the ED observation of the $x = 0.5$ and 0.75 samples did not indicate any sign of the Na/Ca orderings in either short or long range, the drastic change of over 5 orders of magnitude should reflect the influence of the decreasing carrier density.

The small panel in Fig. 5 shows the same data for CaRh_2O_4 in two independent formats, logarithmic ρ vs. $1/T$ (upper, Arrhenius) and $1/T^{0.25}$ (lower, variable range hopping). The data show nearly linear behavior in the latter form, suggesting a hopping conduction mechanism is dominant in CaRh_2O_4 . This result is in contrast to a preliminary band structure calculation on the basis of the single crystal structure data, which suggests a substantial gap at the Fermi level of approximately 1 eV [35]. Even if the data followed the Arrhenius form, the estimated magnitude of the gap would be ~ 32 meV (as indicated by the dotted line). The inconsistency between the calculation and experiment might result from the non-stoichiometry of the polycrystalline sample, which might supply a small amount of extrinsic carriers and lead to the hopping conduction. The dopant feature was also seen in the magnetic and the thermoelectronic properties of CaRh_2O_4 as shown later.

The Seebeck coefficient below 300 K for the solid solution is presented in Fig. 6. The coefficient of the most metallic compound NaRh_2O_4 is small and negative, indicating that the transport is dominated

by n-type carriers. Unfortunately, the small value of the thermopower precludes the rhodate material for any practical applications, as is found in NaCo_2O_4 [28,29]. The Seebeck coefficient increases in magnitude as a function of Ca concentration and reaches a maximum at $x = 0.75$. Combined with the curvature observed and the zero-crossing, the data suggest that both electron and hole carriers contribute to the transport in this system. The concentration (or mobility) of hole-like carriers apparently increases with increasing Ca content. The two-carrier electronic system and a peak at the CaRh_2O_4 composition suggest that single crystal measurements both parallel and perpendicular to the chain direction are needed for a more detailed understanding of the transport properties.

Magnetic susceptibility measured at 10 kOe on cooling is shown in Fig. 7. The fairly metallic compound NaRh_2O_4 shows indeed Pauli-type paramagnetism. At room temperature the susceptibility is $\sim 3 \times 10^{-4}$ emu/mol of Rh and decreases with increasing Ca content; this would indicate the density of states at the Fermi level also decreases. The magnetic susceptibility of CaRh_2O_4 is fairly small and nearly temperature-independent around room temperature. However, it abruptly rises at low temperature. The feature is most pronounced at $x = 0.75$ and disappears at the higher Na concentration. A corresponding enhancement is seen in the M vs. H curve (small panel). The observations are indicative of a possible association between the magnetic enhancement and losing the electrical conductivity. The temperature dependent susceptibility is reminiscent of what is expected for a dilute localized magnetic moment system, as the compounds with low Na content ($< \sim 25\%$) are in fact electrically insulating. The small amount of net carriers may be rather localized and help to produce the dilute magnetic moments. Further studies would be required to improve our understanding of the probable correlation between the magnetic and the transport properties of the Na/Ca solid solution.

The specific heat data were quantitatively analyzed in a well-established way. First, the raw data were plotted as C_p/T vs T^2 as shown in Fig. 8, and then the following form was applied to fit the linear part by a least-squares method:

$$C_v/T = \gamma + 2.4\pi^4 r N_0 k_B (1/\Theta_D^3) T^2,$$

where k_B , N_0 , and r were the Boltzmann constant, Avogadro's constant, and the number of atoms per formula unit, respectively. The two parameters γ (electronic-specific-heat coefficient) and Θ_D (Debye temperature) are material dependent. The analysis is valid in the low-temperature limit ($T \ll \Theta_D$). The difference between C_p and C_v was assumed insignificant in the temperature range studied. The γ and Θ_D values for $\text{Ca}_{1-x}\text{Na}_x\text{Rh}_2\text{O}_4$ were then obtained and plotted in the small panel of Fig. 8. The linear part of the data used in the analysis was $20 \text{ K}^2 < T^2 < 100 \text{ K}^2$ ($4.5 \text{ K} < T < 10 \text{ K}$) for NaRh_2O_4 and $\text{Na}_{0.75}\text{Ca}_{0.25}\text{Rh}_2\text{O}_4$, $60 \text{ K}^2 < T^2 < 100 \text{ K}^2$ ($7.8 \text{ K} < T < 10 \text{ K}$) for $\text{Na}_{0.5}\text{Ca}_{0.5}\text{Rh}_2\text{O}_4$ and $\text{Na}_{0.25}\text{Ca}_{0.75}\text{Rh}_2\text{O}_4$, and $3.4 \text{ K}^2 < T^2 < 100 \text{ K}^2$ ($1.8 \text{ K} < T < 10 \text{ K}$) for CaRh_2O_4 .

The pure Ca sample is electrically insulating, and the γ is, therefore, expected to be zero since the Fermi level would lie in the band gap; however, this is not the case. The CaRh_2O_4 polycrystalline sample has a γ of $2.85(2) \text{ mJ/mol of Rh K}^2$. The small but nonzero γ suggests, as do the other transport measurements, that a small density of in-gap states exist, probably due to the slight off-stoichiometry of the polycrystalline sample. The small characteristic feature at low temperature at $x = 0.75$ is indicative of contributions from dilute localized magnetic moments [36,37]. For NaRh_2O_4 , the γ value was $10.13(2) \text{ mJ/mol of Rh K}^2$. Using these values of γ and χ (approximately $3 \times 10^{-4} \text{ emu/mole of Rh}$), we find the Wilson ratio for NaRh_2O_4 is approximately 2.0 [38], which would suggest the data are somewhat influenced by substantial electron correlations. Further measurements, exploring the correlated behavior in NaRh_2O_4 and closely related compounds, may prove very interesting.

In summary, the sodium rhodate NaRh_2O_4 was synthesized for the first time under extraordinary conditions. The local structure, magnetic, and electrical properties were studied in detail, and investigation by the aliovalent substitution Na/Ca was conducted. The sodium rhodate NaRh_2O_4 was found to be fairly metallic and possibly influenced by substantial electron correlations. The peculiar association of the small amount of electrical carriers and the magnetic moments was suggested for the Na/Ca solid solution. Despite our effort to discover a distinctive feature of the RhO_6 network, neither superconductivity nor an ordered magnetic state was observed above 1.8 K below 70 kOe. Further

studies on high-quality single crystals would help to clarify and develop our understanding of the physical properties and correlated electron behavior of these compounds. Since intriguing properties due to substantial electron correlations are expected, further synthesis and measurement studies are in progress.

ACKNOWLEDGMENT

We wish to thank M. Akaishi (NIMS) for the high-pressure experiment and H. Aoki (NIMS) for the EDS study. We also express gratitude to Dr. R.V. Shpanchenko for helpful discussion. This research was supported in part by the Superconducting Materials Research Project, administrated by the Ministry of Education, Culture, Sports, Science and Technology of Japan, and by Grants-in-Aid for Scientific Research from the Japan Society for the Promotion of Science (16076209, 16340111).

SUPPORTING INFORMATION PARAGRAPH

Powder x-ray profile of NaRh_2O_4 (expanded view), ED patterns, crystallographic information files (CIF), and tables of selected bond distances and angles for NaRh_2O_4 and CaRh_2O_4 . These materials are available free of charge via the Internet at <http://pubs.acs.org>.

References

- [1] Muller-Buschbaum, Hk. *J. Alloys Comp.* **2003**, 349, 49.
- [2] Muller, O.; Roy, R. *The Major Ternary Structural Families*, Springer-Verlag, **1974**, page 55.
- [3] Hill, P.M.; Peiser, H.S.; Rait, J.R. *Acta Crystallogr.* **1956**, 9, 981.
- [4] Wells, A.F. *Structural Inorganic Chemistry, Fifth edition*, Clarendon Press, Oxford **1984**, page 600.
- [5] Irifune, T.; Fujino, K.; Ohtani, E. *Nature* **1991**, 349, 409.
- [6] Darriet, J.; Vidal, A. *Bull. Soc. Fr. Mineral. Cristallogr.* **1075**, 98, 374.
- [7] Zouari, S.; Ranno, L.; Cheikh-Rouhou, A.; Isnard, O.; Pernet, M.; Wolfers, P.; Strobel, P. *J. Alloys Comp.* **2003**, 353, 5.
- [8] Zouari, S.; Ranno, L.; Cheikh-Rouhou, A.; Pernet, M.; Strobel, P. *J. Mater. Chem.* **2003**, 13, 951.
- [9] Ling, C.D.; Neumeier, J.J.; Argyriou, D.N. *J. Solid State Chem.* **2001**, 160, 167.
- [10] Ito, S.; Suzuki, K.; Inagaki, M.; Naka, S. *Mater. Res. Bull.* **1980**, 15, 925.
- [11] Michel, C.; Hervieu, M.; Raveau, B.; Li, S.; Greaney, M.; Fine, S.; Potenza, J.; Greenblatt, M. *Mater. Res. Bull.* **1991**, 26, 123.
- [12] Kolev, N.; Iliev, M.N.; Popov, V.N.; Gospodinov, M. *Solid State Commun.* **2003**, 128, 153.
- [13] Geselbracht, M.J.; Noailles, L.D.; Ngo, L.T.; Pikul, J.H.; Walton, R.I.; Cowell, E.S.; Millange, F.; O'Hare, D. *Chem. Mater.* **2004**, 16, 1153.
- [14] Akimoto, J.; Takei, H. *J. Solid State Chem.* **1989**, 79, 212.
- [15] Anderson, P.W. *The Theory of Superconductivity in the High-Tc Cuprate Superconductors*, Princeton Series in Physics, **1997**.

- [16] Mackenzie, A.P.; Maeno, Y. *Rev. Mod. Phys.* **2003**, *75*, 657.
- [17] Tokura, Y.; Nagaosa, N. *Science* **2000**, *288*, 462.
- [18] Jacob, K.T.; Waseda, Y. *J. Solid State Chem.* **2000**, *150*, 213.
- [19] Skrobot, V.N.; Grebenshchikov, R.G. *Russ. J. Inorg. Chem.* **1989**, *34*, 2127.
- [20] Leiva, H.; Kershaw, R.; Dwight, K.; Wold, A. *Mat. Res. Bull.* **1982**, *17*, 1539.
- [21] Hobbie, K.; Hoppe, R. *Z. Anorg. Allg. Chem.* **1988**, *565*, 106.
- [22] Kanke, Y.; Akaishi, M.; Yamaoka, S.; Taniguchi, T. *Rev. Sci. Instrum.* **2002**, *73*, 3268.
- [23] Yamaoka, S.; Akaishi, M.; Kanda, H.; Osawa, T.; Taniguchi, T.; Sei, H.; Fukunaga, O. *J. High Pressure Inst. Jpn.* **1992**, *30*, 249.
- [24] Muller-Buschbaum, Hk.; Frerichs, D. *J. Alloys Comp.* **1993**, *199*, L5.
- [25] SMART, SAINT+, and SADABS packages, Bruker Analytical X-ray Systems Inc., Madison, WI, **2002**.
- [26] Sheldrick, G.M. SHELXL97 Program for the Solution and Refinement of Crystal Structures, University of Göttingen, Germany, **1997**.
- [27] Larson, A.C.; Von Dreele, R.B. *Los Alamos National Laboratory Report* No. LAUR086-748, **1990**.
- [28] Terasaki, I.; Sasago, Y.; Uchinokura, K. *Phys. Rev. B* **1997**, *56*, 12685.
- [29] Wang, Y.Y.; Rogado, N.S.; Cava, R.J.; Ong, N.P. *Nature* **2003**, *423*, 425.
- [30] Chen, B.H.; Walker, D.; Scott, B.A. *Chem. Mater.* **1997**, *9*, 1700.
- [31] Kumiyama, K.; Steinfinkl, H. *Inorg. Chem.* **1968**, *7*, 1762.
- [32] Shannon, R.D. *Acta. Cryst. A* **1976**, *32*, 751.

- [33] Bertaut, E.F.; Blum, P. *J. Phys. Radium* **1956**, *17*, 517.
- [34] Bertaut, E.F.; Blum, P. *Acta Crystallogr.* **1956**, *9*, 121.
- [35] Arai, M. unpublished.
- [36] Wada, H.; Hada, M.; Ishihara, K.N.; Shiga, M.; Nakamura, Y. *J. Phys. Soc. Jpn.* **1990**, *59*, 2956.
- [37] Loram, J.W.; Chen, Z. *J. Phys. F: Met. Phys.* **1983**, *13*, 1519.
- [38] Wilson, K.G. *Rev. Mod. Phys.* **1975**, *47*, 773.

Table I. Crystallographic data and structure refinement for NaRh₂O₄

empirical formula	NaRh ₂ O ₄
formula weight	292.798
temperature	295 K
neutron wavelength	1.5396(1) Å
diffractometer	BT-1 at the NIST Center for Neutron Research
two theta range used	3° – 168° in 0.05° steps
crystal system	orthorhombic
space group	<i>Pnma</i>
lattice constants	$a = 9.0026(4)$ Å $b = 3.0461(2)$ Å $c = 10.7268(5)$ Å
volume	294.16(3) Å ³
<i>Z</i>	4
density (calculated)	6.611 g/cm ³
observations	2999
<i>R</i> factors	4.88 % (<i>R</i> _{wp}) 3.91 % (<i>R</i> _p)
Refinement software	GSAS

Table II. Atomic coordinates and isotropic displacement parameters for NaRh₂O₄ at 295 K.

Atom	site	x	y	z	$100U_{\text{iso}} (\text{\AA}^2)$	n
Na	4c	0.7629(6)	1/4	0.6577(6)	1.40(12)	1
Rh1	4c	0.4137(4)	1/4	0.1029(3)	0.590(47)	1
Rh2	4c	0.4431(4)	1/4	0.6162(3)	0.590(47)	1
O1	4c	0.1982(4)	1/4	0.1579(3)	0.759(69)	1
O2	4c	0.1166(3)	1/4	0.4797(3)	0.729(77)	1
O3	4c	0.5319(4)	1/4	0.7862(3)	0.832(68)	1
O4	4c	0.4178(4)	1/4	0.4295(3)	0.598(69)	1

The thermal parameters of Rh atoms were grouped and refined together.

Table III. Crystallographic data and structure refinement for CaRh₂O₄

empirical formula	CaRh ₂ O ₄
formula weight	309.90
temperature	298 K
wavelength	MoK α (0.71069 Å)
crystal system	orthorhombic
space group	<i>Pnma</i> (no. 62)
unit cell dimensions	$a = 9.0354(3)$ Å $b = 3.0340(1)$ Å $c = 10.7062(3)$ Å
cell volume	293.49(2) Å ³
Z	4
density, calculated	7.014 g/cm ³
crystal size (mm)	0.04×0.02×0.1
<i>h k l</i> range	$-20 \leq h \leq 18$, $-5 \leq k \leq 6$, $-23 \leq l \leq 23$
$2\theta_{\max}$	104.27
linear absorption coeff.	12.63 mm ⁻¹
absorption correction	multi-scan (SADABS; Bruker, 1999)
T_{\min}/T_{\max}	0.5101/0.3815
no. of reflections	9055
R_{int}	0.0326
no. independent reflections	1833
no. observed reflections	1583 [$F_o > 4\sigma(F_o)$]
$F(000)$	568
<i>R</i> factors	3.07 % (R_p) 8.73 % (R_{wp})
weighting scheme	$w = 1/[\sigma^2(F_o^2) + (0.0551P)^2 + 0.02P]$, $P = (\text{Max}(F_o^2) + 2F_c^2)/3$
diff. Fourier residues	[-2.35, 2.66] e/Å ³
Refinement software	SHELXL-97

Table IV. Atomic coordinates and anisotropic displacement parameters for CaRh_2O_4 at 298 K.

Atom	site	x	y	z	$100U_{\text{eq}} (\text{\AA}^2)$	n
Ca	4c	0.23807(8)	1/4	0.34015(7)	1.228(11)	1
Rh1	4c	0.08643(3)	1/4	0.60010(2)	0.569(5)	1
Rh2	4c	0.05631(3)	1/4	0.11510(2)	0.536(5)	1
O1	4c	0.3015(3)	1/4	0.1579(3)	0.702(28)	1
O2	4c	0.3825(2)	1/4	-0.0236(2)	0.526(26)	1
O3	4c	0.4688(3)	1/4	0.2114(2)	0.598(27)	1
O4	4c	0.0850(2)	1/4	-0.0726(2)	0.528(27)	1
Atom	$100U_{11}$	$100U_{22}$	$100U_{33}$	$100U_{23}$	$100U_{13}$	$100U_{12}$
Ca1	0.72(2)	2.16(3)	0.808(19)	0	0.004(16)	0
Rh1	0.514(8)	0.677(8)	0.515(7)	0	-0.016(5)	0
Rh2	0.512(8)	0.553(8)	0.543(7)	0	-0.022(5)	0
O1	0.35(6)	0.76(8)	1.00(7)	0	0.03(6)	0
O2	0.33(6)	0.77(7)	0.48(6)	0	0.02(5)	0
O3	0.60(7)	0.75(7)	0.45(6)	0	-0.15(5)	0
O4	0.37(6)	0.56(7)	0.65(6)	0	-0.04(5)	0

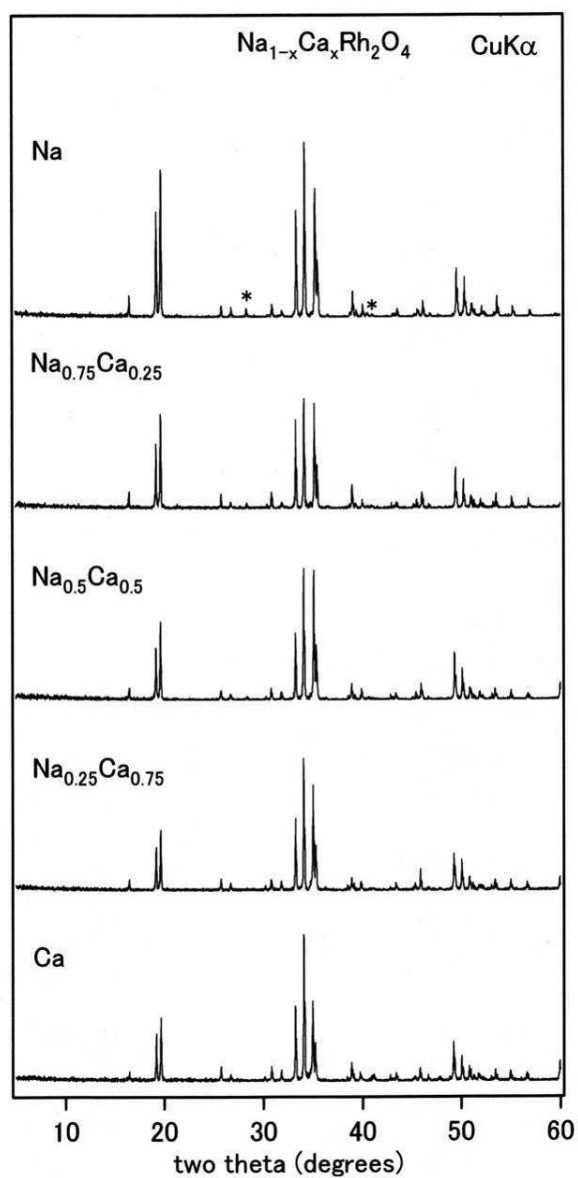


Fig1. Powder x-ray diffraction profile of the $\text{Na}_{1-x}\text{Ca}_x\text{Rh}_2\text{O}_4$ samples, measured at room temperature. Star marks indicate peaks for KCl. For clarity hkl indexes are not shown for here, but an expanded view with the indexes is presented in a supporting information file.

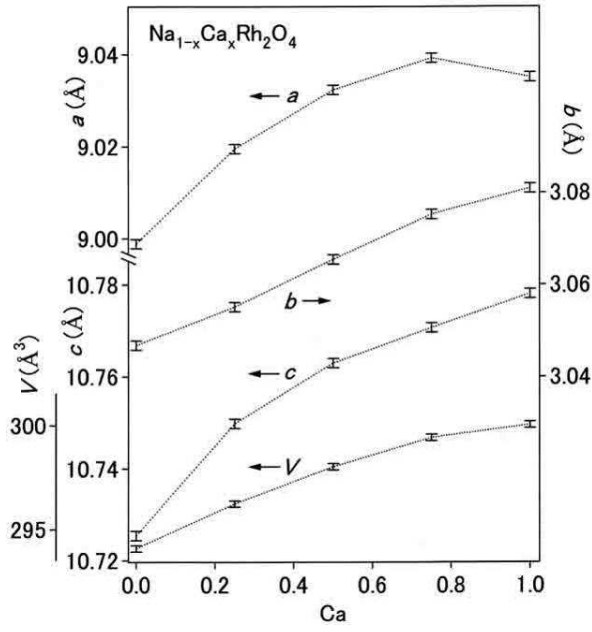


Fig2. Orthorhombic unit-cell parameters and the unit-cell volume of $\text{Na}_{1-x}\text{Ca}_x\text{Rh}_2\text{O}_4$, measured at room temperature by an X-ray diffraction method.

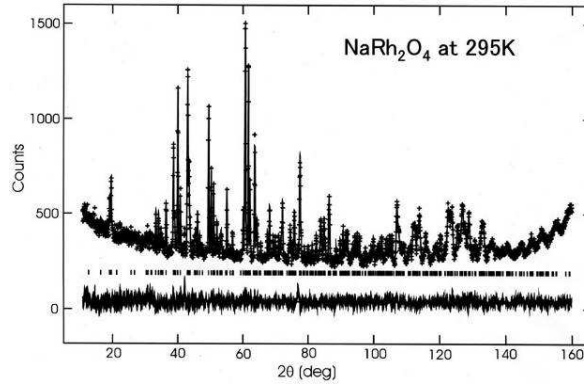


Fig3. Neutron diffraction profile of the NaRh_2O_4 sample (~1 gram), measured at 295 K. Vertical bars indicate allowed Bragg reflections on the basis of the $Pnma$ structure. The difference between the best computed profile (solid lines) and the raw data (crosses) is shown below the bars column.

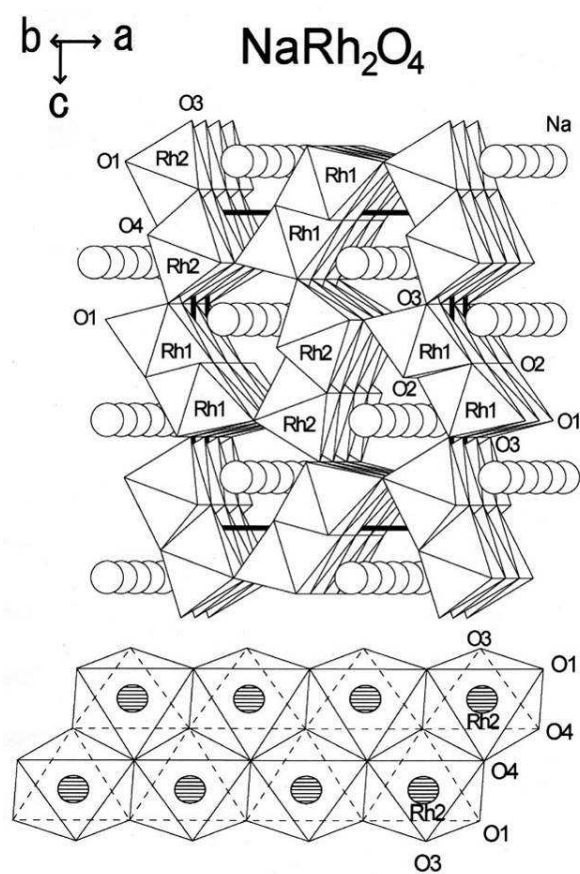


Fig4. Structure view of NaRh_2O_4 . Bold lines signify the orthorhombic unit cell. Bottom figure indicates a part of the double chain along the b -axis.

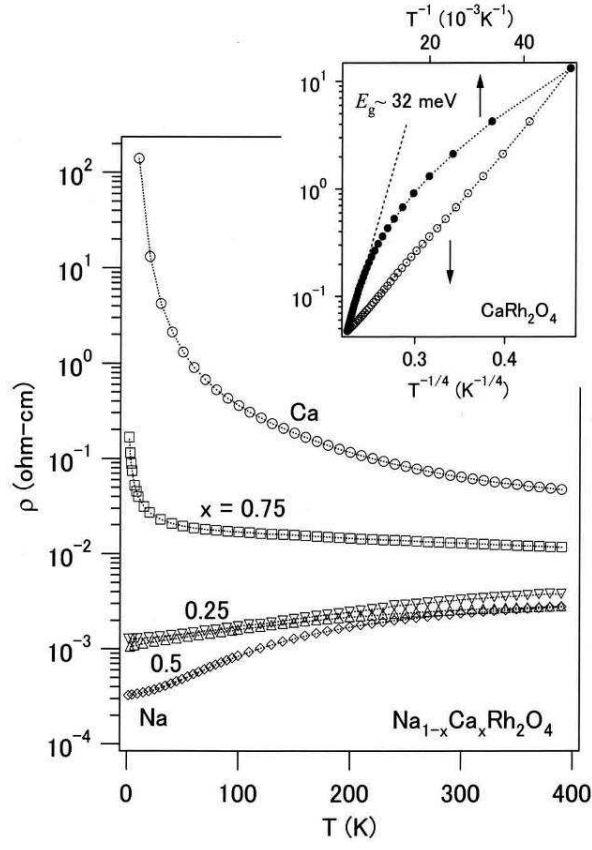


Fig5. Temperature and composition dependence of the electrical resistivity of the polycrystalline $\text{Na}_{1-x}\text{Ca}_x\text{Rh}_2\text{O}_4$. (Top panel) Comparison between the two plots of the data for CaRh_2O_4 .

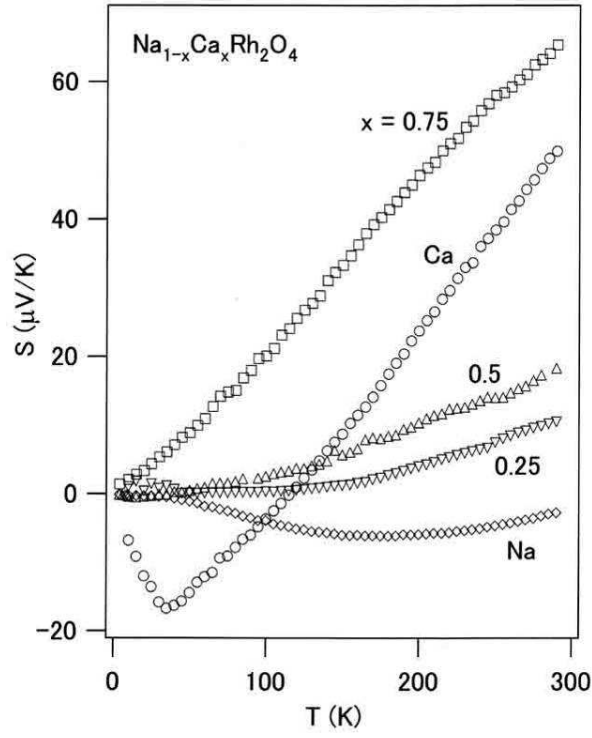


Fig6. Thermoelectric power of the polycrystalline $\text{Na}_{1-x}\text{Ca}_x\text{Rh}_2\text{O}_4$.

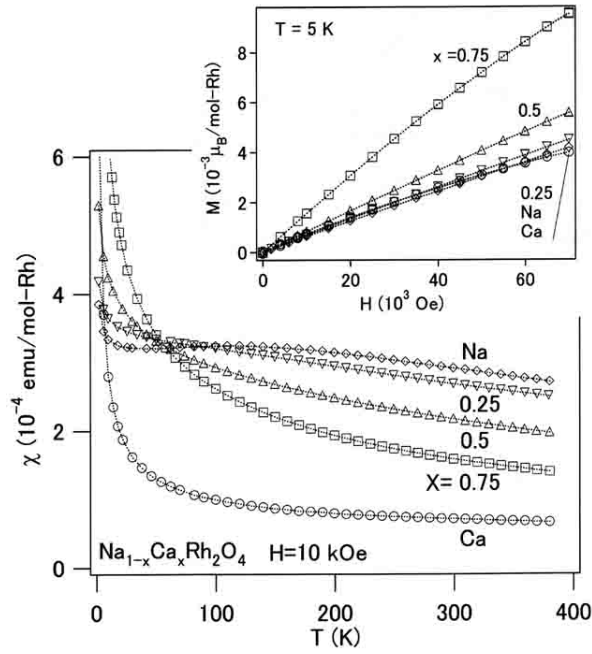


Fig7. Temperature dependence of the magnetic susceptibility of the polycrystalline $\text{Na}_{1-x}\text{Ca}_x\text{Rh}_2\text{O}_4$, measured at 10 kOe on cooling, and applied field dependence of the magnetization at 5 K (top panel).

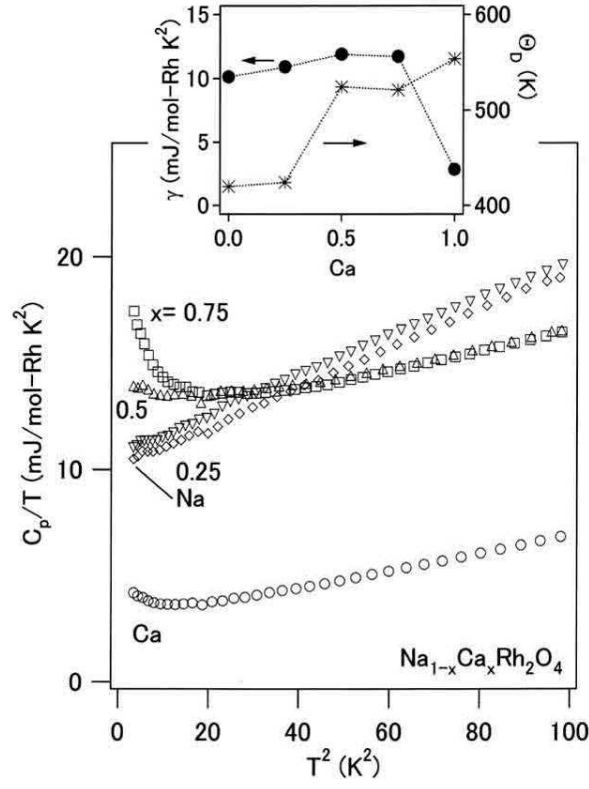


Fig8. Specific heat of the polycrystalline $\text{Na}_{1-x}\text{Ca}_x\text{Rh}_2\text{O}_4$. Small panel shows evolution of γ (electronic-specific-heat coefficient) and Θ_D (Debye temperature), estimated from the data. Error bars of the γ and Θ_D points are smaller than the marker size.